

## THE SMALL-SCALE INTERSTELLAR DUST DISTRIBUTION

ALEJANDRO CLOCCHIATTI<sup>a)</sup> AND HUGO G. MARRACO<sup>b)</sup>

Facultad de Ciencias Astronómicas y Geofísicas, Universidad Nacional de La Plata, Programa de Fotometría y Estructura Galáctica, Consejo Nacional de Investigaciones Científicas y Técnicas, Argentina

Received 7 April 1986; revised 30 June 1986

## ABSTRACT

The statistical distribution of interstellar dust at scale distances of a few parsecs is studied in the direction of the cluster NGC 2516 (C0757 — 607). Models composed of individual clouds that match the cluster's mean color excess and its true dispersion are built. The characteristics of the models are described and their average properties are presented. The interstellar-matter structural function is computed from the models and compared to that observed for the cluster. It is concluded that (a) best fits are obtained with models using clouds having an average size of 3 pc if the clouds are clumped together in a hierarchical way, and (b) these hierarchical complexes cannot be placed at random, but must have some kind of periodicity in their locations.

## I. INTRODUCTION

The existence of small-scale structure in the standard interstellar dark medium is presently noncontroversial; however, little is known concerning the statistical features of its individual constituents, namely dark clouds, and their distribution.

The oversimplified model proposed by Münch (1952) gives only illustrative values for the cloud parameters. Since the paper by Chandrasekhar and Münch (1952) that introduced the concept of angular-correlation coefficients for interstellar reddening, Serkowski (1958), Scheffler (1967), Krzeminski (1967), and Serkowski (1968) have computed the microscale of the fluctuations in space density of interstellar dust. The collection of information about the small-scale distribution of dark interstellar matter seems to have ceased during the past decade.

The first paper by Serkowski provides the basis for a method of analyzing the statistical fluctuations of the projected density. This method was first used by Feinstein and Marraco (1971), and further developed by Clocchiatti and Marraco (1986, hereafter referred to as Paper I). Its main characteristics consist in calculating the interstellar-matter structural function (hereafter referred to as the IMSF), defined by Serkowski (1958), in a reliable way, and in using it to find information about the distribution of the interstellar dust. Traditionally the IMSF has been used to derive the microscale of the density fluctuations; the hope of our method is to use it to find some other characteristics of the dust distribution, as for instance, details like periodicities and/or clumping in the cloud distribution.

In Paper I the utility of the IMSF as an instrument for deriving statistical features of the interstellar dust was studied. Its behavior in some ideal models was shown, and the authors concluded that the IMSF is a sensitive parameter for testing the regular features of the interstellar-dust distribution. In the present paper we build a static model of the interstellar-dust distribution, and compute the IMSF for test stars belonging to an open cluster in the region under study. Our model and the observations are compared using the mean and the dispersion of the color excess. The comparison between the observed IMSF and the model IMSF gives the additional information sought.

<sup>a)</sup> On a fellowship from CONICET.

<sup>b)</sup> Member of the Carrera del Investigador Científico del Consejo Nacional de Investigaciones Científicas y Técnicas (CONICET).

Section II deals with the computation of the IMSF from the observed reddenings. Section III describes the models and analyzes the free variables and how to reduce their degree of freedom. Section IV describes the results obtained in modeling the region of the open cluster NGC 2516. Section V discusses the results. Finally, Sec. VI summarizes our conclusions.

## II. THE OBSERVED IMSF

The open cluster NGC 2516 is located in the Carina region, at a distance of about 400 pc (Feinstein *et al.* 1973a). According to Lucke (1978), reddening in this direction is low, strengthening the hypothesis that dark matter has a normal behavior in this region.

To obtain the IMSF for NGC 2516, 47 stars were used. The photometric data, obtained from Cox (1955), Evans (1961), Dachs (1970), Eggen (1972), and Feinstein *et al.* (1973a), were reduced (Marraco 1975) to the system of Feinstein *et al.* (1973a). To ensure precision in the unreddened colors, stars of spectral type earlier than A0 were chosen. The computed values for the mean color excess and its dispersion are 0.119 and 0.0257, respectively. To avoid the effect of the intrinsic reddening dispersion (i.e., the contribution to the reddening dispersion due to causes other than the interstellar-matter distribution) the method proposed by Feinstein *et al.* (1973a) was used. The estimated extrinsic reddening dispersion is 0.016 mag. The corresponding value for the true reddening dispersion is 0.020 mag, with an estimated error of 0.003 mag. With these values, we are able to correct the IMSF and normalize it. No further comments about the properties and way of computing the IMSF will be made in the present paper.

The resulting normalized IMSF is shown in Fig. 1. Its prominent features are as follows.

(a) There is an oscillating behavior between 1.7 and 4.2 pc, with maxima at 1.7 and 3.3 pc and minima at 2.5 and 4.2 pc. According to Paper I this reveals that the interstellar dark matter has some separate concentrations, and that typical distances for their distribution and size are on the order of 1.7 pc.

(b) The high gradient in the neighborhood of 1 pc is related to the average distances for color-excess fluctuations of about 1.61 pc.

Both values are in reasonable agreement with the micro-

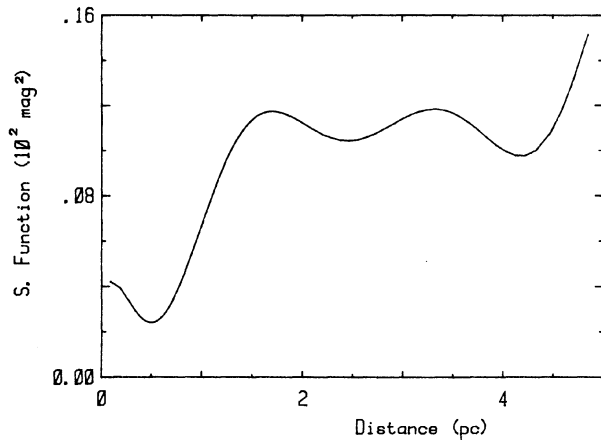


FIG. 1. The IMSF of NGC 2516. The abscissa gives separation in parsecs, and the ordinate gives one hundred times the square of the difference in excess in magnitudes.

scale for the density fluctuations computed by Serkowski (1968, and references therein).

### III. THE MODEL

The conclusions of the preceding section may be used to set up a hypothetical model of the interstellar-dust distribution in the direction of NGC 2516. It is apparent that the model must have concentrations and, for simplicity, spherically symmetric concentrations of dust were chosen. It is clear that the spherical concentrations may be used to build arbitrarily shaped concentrations by suitably arranging them. However, it should be noted that they must not be regarded in a deterministic sense. Their role is similar to the role of the spheres used in modeling interstellar grains for stellar reddening. In other words, the cloud parameters will have meaning only from a statistical point of view.

The following dust-density distribution for each of these clouds is assumed:

$$\rho_D(r) = \rho_D^0 e^{-(r/r_0)^2}, \quad (1)$$

where  $r$  is the distance from the cloud center,  $\rho_D^0$  is the central dust density of the cloud, and  $r_0$  is the characteristic radius representative of the size.

Using Eq. (1) it is possible to find the color excess due to the cloud for a star located at a projected distance  $p$  from its center. This is

$$E_{B-V}(p) = \sqrt{\pi} C_{B-V} r_0 \rho_D^0 e^{-(p/r_0)^2}, \quad (2)$$

where  $C_{B-V} = \kappa_B - \kappa_V$  is the differential absorption constant per unit mass. To fix its value, it is necessary to adopt a dust model and make use of its photometric characteristics. We assume the model proposed by Mathis *et al.* (1981) is valid. Using the extinctions presented in this work, we compute  $\kappa_B = 4.48 \text{ mag cm}^2 \text{ g}^{-1}$ ,  $\kappa_V = 3.36 \text{ mag cm}^2 \text{ g}^{-1}$ , and  $C_{B-V} = 1.12 \text{ mag cm}^2 \text{ g}^{-1}$ . The  $\kappa_V$  value is about 1.4 times greater than the value adopted by Feinstein *et al.* (1973b) for the  $\eta$  Carinae region. However, the dust models used are different.

Using Eq. (1), one may obtain the total mass of the cloud:

$$M = \pi^{3/2} \rho_T^0 r_0^3, \quad (3)$$

where  $\rho_T^0$  is the sum of the dust and gas central densities. To write this equation, we assumed that the gas and dust are

homogeneously mixed. This is a fairly strong assumption because it is known (Reddish 1971) that under certain conditions of the radiation field interstellar matter will separate into dust and gas phases on time scales of roughly one million years. However, the region under study in the present work is completely free of strong radiative fields, so that the supposition of homogeneity seems to be reasonable.

The mass, with the additional assumption of a fixed gas to dust mass ratio, may replace one of the two variables involved in Eq. (1). The mass was preferred because it has a more direct physical interpretation and because some authors give mass distribution functions for the interstellar clouds. This allows a direct comparison of results.

A third descriptive variable is the temperature of the cloud gas that is responsible for the thermodynamic and dynamic behavior of the cloud. Finally, the chemical composition will be chosen.

According to the previous definitions, and once the chemical composition is fixed, there are three variables that describe the physical state of a cloud, and two of them are independent. However, it is intuitive to think that one variable cannot have a completely arbitrary value, independent of the others (for example, arbitrary large size and density), and describe an acceptable cloud for the region under study. There is no other equation similar to Eq. (3) connecting the three variables and independent of it that allows us to reduce the problem to one independent variable. However, there are several conditions that the clouds must satisfy and that give mathematical limits to them. These conditions only involve two variables each, and may be classified in two groups: (a) observational conditions; (b) dynamical conditions.

The first class of conditions comes from a selection effect of the IMSF. On the one hand, the observations give reddenings and the information comes from differences between them. On the other hand, the reddenings are known only in the projected positions of the cluster stars. Hence, the clouds must contribute to the individual reddening of the stars and to the differential reddening of the group. From these considerations it is possible to find four conditions that eliminate excessively thin, dense, compact, or extended clouds from the model. They depend upon the minimum and maximum color excess assigned to one cloud, on the minimum and maximum projected distance between two stars of the cluster, and the minimum difference in color excess that can be detected. The second class of conditions requires that the individual clouds be stable against gravitational collapse and thermal disruption. There are two such conditions, and they depend upon the gas temperature, mean molecular weight, and density profile of the clouds. All the conditions together define a range of useful clouds for the model.

Each of the limits described above divides the  $(\rho_T^0, r_0)$  plane in two regions. The behavior of the limits is shown in Fig. 2.

The distribution of the clouds in the  $(\rho_T^0, r_0)$  plane is obtained by imposing the following generic distribution on the independent variables:

$$N(v) dv = K v^{-\alpha} dv, \quad (4)$$

where  $v$  represents  $M$  or  $\rho_T^0$ ,  $K$  is a normalization constant, and  $\alpha$  is a parameter. Finally, the projected distribution of the clouds in the sky must be chosen. According to Lucke (1978), most of the interstellar dust seen projected against NGC 2516 lies in the immediate neighborhood of this cluster. Due to this fact we treated the locations of the cloud

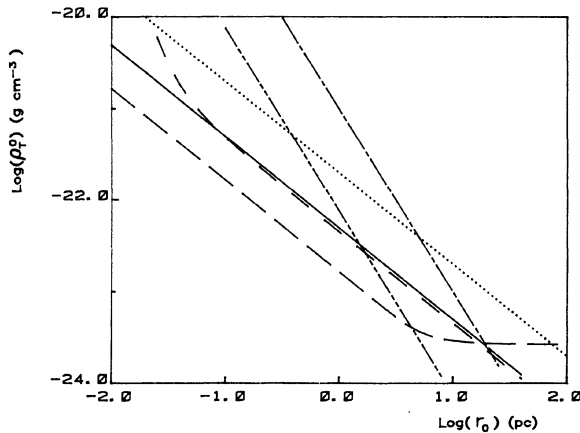


FIG. 2. Acceptable cloud region. The abscissa gives the logarithm of the typical radius in parsecs, and the ordinate gives the logarithm of the central density in  $\text{g}/\text{cm}^3$ . Solid line: limit of thin clouds (lower limit), short dashed line: limit of compact clouds (lower limit), long dashed line: limit of extended clouds (lower limit), dashed double dot line: limit of gravitational collapse for the coldest clouds (lower limit), dashed single dot line: limit of thermal disruption for the hottest clouds (upper limit), dotted line: limit of opaque clouds (upper limit).

centers in a two-dimensional space, disregarding any consideration of distance.

To fix the limits for the useful cloud region, six values must be chosen; these values will be parameters of the model. The distribution of the masses and central densities adds two more parameters. And finally, to fix the projected distribution of clouds in the plane of the sky at least two more parameters are necessary.

In fact, to build one model we need to fix ten parameters. It is apparent that most of them must remain fixed, in order to make it possible to treat the problem. We do not have *a priori* reasons to impose any distribution for the clouds in the rather small region under study. Accordingly, we use uniform distributions of the clouds' centers. This means that the clouds will be randomly located in the plane of the sky. The minimum color excess that may be detected was fixed at 0.01 mag. The mean molecular weight was fixed, following McKutcheon (1982), as  $\mu = 2.33$ . For the maximum and minimum gas temperature, we use the typical values 13 and 3 K, respectively. To fix the upper and lower color excess allowed for one cloud we can use the generic conclusions of Paper I and the previous section. In this sense, we should not include clouds that can produce more than the total amount

of observed reddening. It is reasonable to think that we need several clouds to match the behavior of the IMSF presented in the above section. Hence, we impose on every cloud a central color excess [given by Eq. (2) with  $p = 0$ ] that must be less than the observed mean. This will ensure the presence of several clouds in the region to reach the mean color excess for the cluster. With regard to the minimum color excess, we must be sure that each cloud has its own detectable photometric effect. However, there are no general considerations that allow us to fix quantitatively such an effect. On the one hand, the minimum excess must not be too small or the clouds will tend to be very thin and their effect will be similar to a continuous diffuse medium. On the other hand, if the minimum excess is too large the reddening dispersion will increase excessively. We fix the value for the minimum as 0.03 mag. Table I summarizes the adopted fixed parameters, and Table II gives the resulting limits for densities, typical radii, and masses of the acceptable clouds. The minimum mass presented in Table II agrees reasonably with the one found by Bhatt (1984) in the Taurus complex. The minimum size agrees fairly well with the minimum radius that a more detailed analysis provides (Knude 1981, and references therein). Finally, the parameters which fix the distribution of masses and central densities are kept as free parameters of the model.

To build a model based on the above assumptions, we began by generating an individual cloud [i.e., two descriptive parameters following the generic distribution (4)] and test its location in the  $(\rho_0^0, r_0)$  plane. If the cloud falls within the permitted range of parameters, a random position in the sky plane is generated and assigned to the cloud. Later, we test the photometric effect on the stars of the cluster and, if it is an observable one, the cloud is kept as a model cloud. These steps are repeated until the mean color excess of NGC 2516 is approximately matched. The resulting set of clouds and positions is called a model of the region. To avoid the dependence on the "seed" numbers we generate 20 models for each pair of free parameters  $\alpha$  and  $\beta$  and analyze the mean values of the interesting quantities (hereafter,  $\alpha$  will be the mass distribution function exponent, and  $\beta$  will be the exponent of the central density distribution function). The values tested for the  $\alpha$  parameter are  $-2.5$ ,  $-2.0$ ,  $-1.5$ , and  $-1.0$ , and for  $\beta$   $-3.0$ ,  $-2.5$ ,  $-2.0$ ,  $-1.5$ , and  $-1.0$ .

#### IV. RESULTS

##### a) Cloud Characteristics and Reddening Dispersion

Figure 3(a) shows a contour plot of the mean dispersion of color excess versus the parameters  $\alpha$  and  $\beta$ . It is clear that

TABLE I. Fixed parameters adopted.

(a) Observational conditions	
Maximum central color excess admitted for one cloud (mag)	0.120
Minimum central color excess admitted for one cloud (mag)	0.30
Minimum difference of color excess to be detected (mag)	0.010
Maximum distance for computing color-excess differences (pc)	6.1
Minimum distance for computing color-excess differences (pc)	0.1
Differential absorption between $B$ and $V$ bands (mag $\text{cm}^2 \text{g}^{-1}$ )	$1.12 \times 10^4$
(b) Dynamical conditions	
Mean molecular weight of the cloud material (AMU)	2.33
Maximum mean temperature for the cloud gas (K)	13
Minimum mean temperature for the cloud gas (K)	3
Gas to dust mass ratio	0.01

TABLE II. Physical limits for the clouds.

	Minimum	Maximum
Mass ( $M_{\odot}$ )	2.3	1584
Central density ( $\text{g}/\text{cm}^3$ )	$2.51 \times 10^{-24}$	$5.24 \times 10^{-22}$
Typical radius (pc)	0.38	19.7

## Notes to TABLE II

The limiting values of mass, central density, and typical radius (representative of the size) for acceptable clouds. These values are reached for the clouds at the upper left-hand and lower right-hand corners of the acceptable cloud region (Fig. 2).

there are some pairs of these parameters that match the dispersion and mean color excess of NGC 2516. We do not have *a priori* reasons to prefer one of them. However, it is interesting to point out that the values of  $\alpha$  used are close to those proposed by some authors for the mass distribution functions of dark clouds (Reddish 1971; Bhatt 1984, and references therein).

Variations in the dispersion are related to variations in the physical characteristics of the clouds and their distribution in the  $(\rho_T^0, r_0)$  plane. Figures 3(b)–3(f) show the behavior of the mean mass, central density, typical radius, central

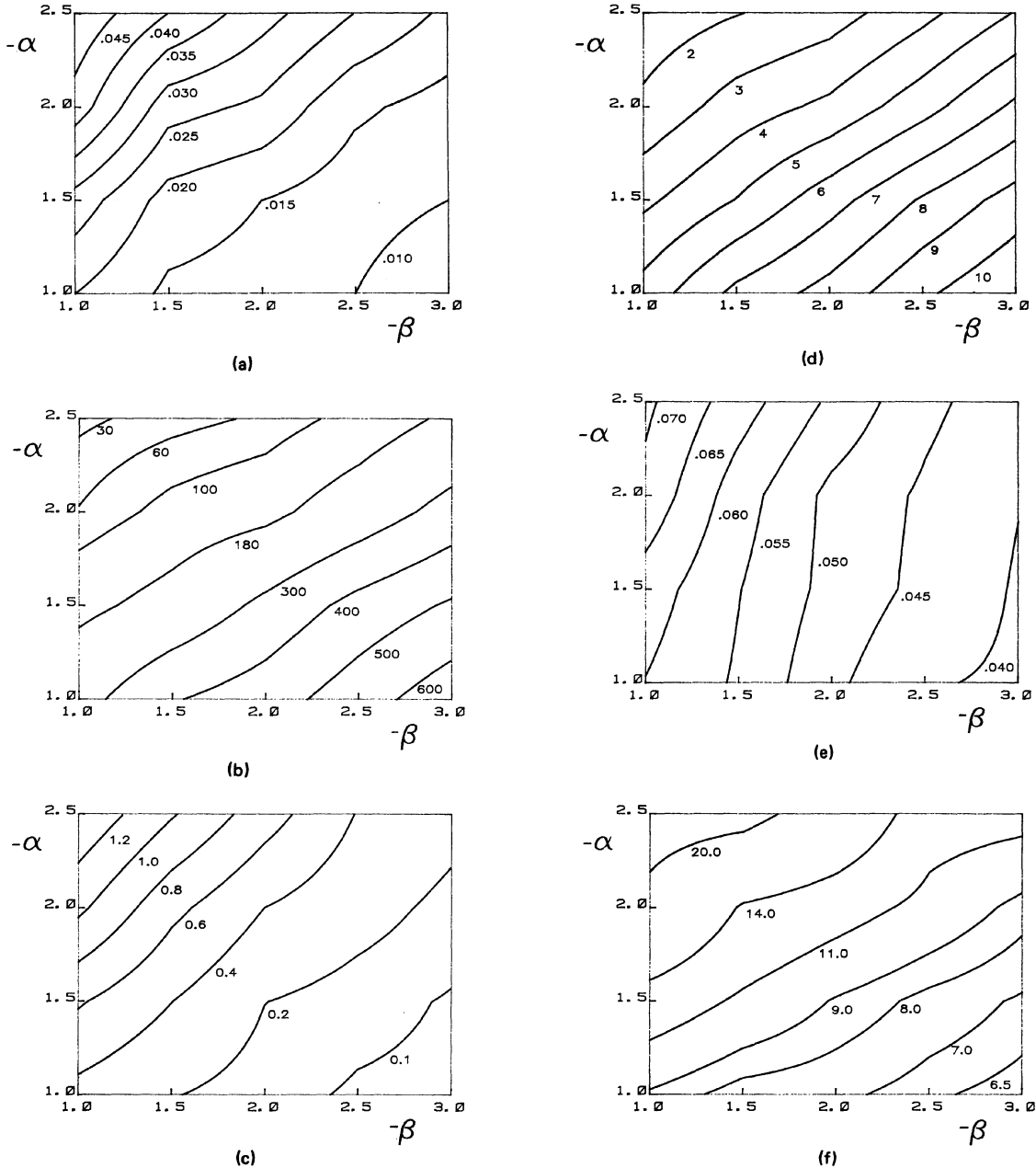


FIG. 3. (a) Contour plot of the mean reddening dispersion of the models versus the parameters  $\alpha$  and  $\beta$ . The contour values are given to the right of each contour. The units are magnitudes. (b) Same as Fig. 3(a), for the mean mass of the clouds. Units are solar masses. (c) Same as Fig. 3(a), for the mean central density. Units are  $1 \times 10^{-22} \text{g}/\text{cm}^3$ . (d) Same as Fig. 3(a), for the mean typical radius. Units are parsecs. (e) Same as Fig. 3(a), for the mean central excess. Units are magnitudes. (f) Same as Fig. 3(a), for the mean number of clouds per model.

TABLE III. Mean results for the models.

(1)	(2)	(3)	(4)	(5)	(6)	(7)	(8)	(9)	(10)	(11)	(12)	(13)
-1.0	-1.0	0.339	0.028	5.4	0.3	262	20	0.060	0.002	0.020	0.002	8.8
-1.0	-1.5	0.205	0.004	7.3	0.1	401	8	0.053	0.001	0.014	0.003	7.4
-1.0	-2.0	0.133	0.011	8.4	0.3	454	28	0.046	0.001	0.013	0.002	7.2
-1.0	-2.5	0.086	0.006	9.8	0.3	556	32	0.040	0.001	0.010	0.001	6.6
-1.0	-3.0	0.074	0.005	10.9	0.3	662	33	0.039	0.001	0.006	0.001	6.3
-1.5	-1.0	0.623	0.048	3.8	0.2	154	14	0.063	0.002	0.028	0.002	12.6
-1.5	-1.5	0.340	0.039	5.0	0.1	222	4	0.054	0.001	0.018	0.002	10.6
-1.5	-2.0	0.203	0.015	6.6	0.3	325	24	0.048	0.001	0.015	0.001	8.9
-1.5	-2.5	0.136	0.011	8.1	0.3	435	28	0.044	0.001	0.012	0.001	7.6
-1.5	-3.0	0.090	0.006	9.4	0.3	515	31	0.039	0.001	0.010	0.001	6.9
-2.0	-1.0	1.044	0.051	2.2	0.1	62	6	0.069	0.001	0.043	0.002	18.8
-2.0	-1.5	0.654	0.049	3.5	0.2	120	11	0.057	0.001	0.027	0.002	13.6
-2.0	-2.0	0.399	0.034	4.2	0.2	154	13	0.049	0.001	0.024	0.001	12.0
-2.0	-2.5	0.264	0.031	5.6	0.3	239	19	0.044	0.001	0.016	0.002	10.4
-2.0	-3.0	0.156	0.017	7.2	0.3	338	24	0.040	0.001	0.013	0.002	8.5
-2.5	-1.0	1.371	0.052	1.4	0.1	22	2	0.071	0.001	0.049	0.002	21.9
-2.5	-1.5	1.019	0.047	2.0	0.1	45	5	0.062	0.001	0.040	0.002	21.5
-2.5	-2.0	0.686	0.039	2.5	0.1	67	7	0.054	0.001	0.032	0.002	17.5
-2.5	-2.5	0.388	0.026	3.7	0.2	122	13	0.046	0.001	0.025	0.002	12.1
-2.5	-3.0	0.257	0.019	5.1	0.2	199	18	0.042	0.001	0.019	0.002	11.8

Notes to TABLE III

Grid of the average characteristics of the models. Column 1 gives the exponent  $\alpha$ , column 2 gives the exponent  $\beta$ . Columns 3 and 4 give the mean central density of the clouds and its error, respectively; the units are  $1 \times 10^{-22}$  g/cm<sup>3</sup>. Columns 5 and 6 give the mean typical radius of the clouds and its error; the units are parsecs. Columns 7 and 8 give the mean total mass of the clouds and its error; the units are solar masses. Columns 9 and 10 give the mean central excess of the clouds and its error; the units are magnitudes. Columns 11 and 12 give the mean reddening dispersion of the models and its error; the units are magnitudes. Column 13 gives the mean number of clouds per model.

excess, and average number of clouds per model, respectively. Table III summarizes their values at the grid points named in Sec. III.

It is easy to understand the contour levels by recalling the meaning of the parameters  $\alpha$  and  $\beta$ , and looking at Fig. 2. When  $\alpha$  is increased, the distribution of cloud masses tends to become more uniform, the models tend to have larger but less dense clouds, the central excesses fall (because the decrease in the central density is not compensated by an increase in the typical radius), and the average number of clouds per model shows a slight decrease. Accordingly, the dispersion in color excess falls.

Logically, this behavior is strengthened by the decrease in the exponent  $\beta$ , or partially compensated for its growth.

Hence, the contour levels run diagonally. Figures 4(a) and 4(b) show the features of the cloud distribution in the useful cloud region with parameters  $\alpha = -2.50, \beta = -1.00$  and  $\alpha = -1.00, \beta = -2.00$ . These plots show that the clouds tend to concentrate in positions close to or far from a given limit, depending upon the values of  $\alpha$  and  $\beta$ . Hence, one limit can be critical in a region of the  $\alpha, \beta$  plane and noncritical in the remaining regions. It is interesting to note that the contour levels for some different quantities are almost coincident. Hence, we can conclude that most of the models that statistically match the reddening dispersion of NGC 2516 have some common features. These are a mean mass for each cloud of about  $200 M_{\odot}$ , a mean central density between approximately  $3.0 \times 10^{-23}$  and  $4.0 \times 10^{-23}$  g/cm<sup>3</sup>, a mean

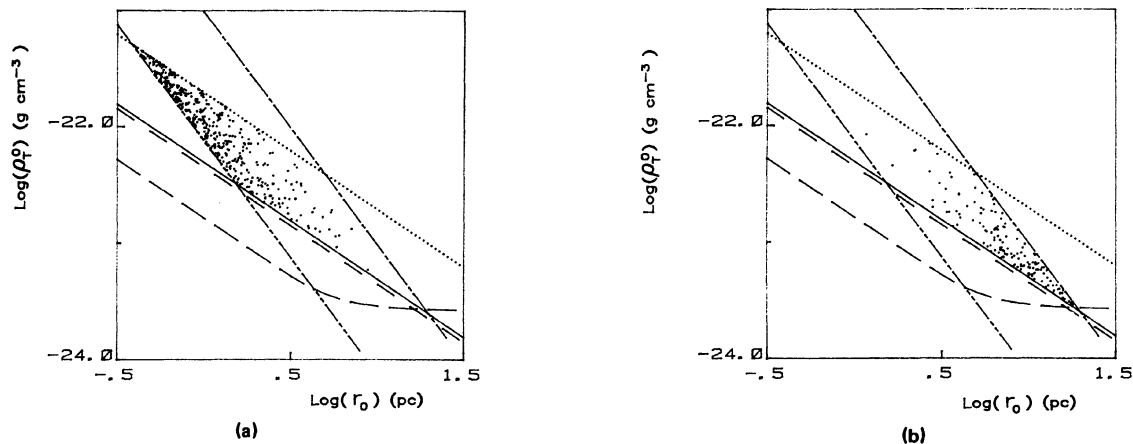


FIG. 4. (a) Distribution of the model clouds in the acceptable cloud region. The units are the same as in Fig. 2. The dots represent the 438 clouds belonging to 20 models with parameters  $\alpha = -2.5, \beta = -1.0$ . (b) Same as Fig. 4(a), but here are represented 144 clouds for 20 models with parameters  $\alpha = -1.0, \beta = -2.0$ .

typical radius of about 5 pc, and a mean number of clouds per model of about 10. The contour levels for the central color excess are not similar to the others. For this reason, the mean central excesses of the clouds on contour level 0.020 fall between approximately 0.040 and 0.060 mag.

### b) The IMSF

We computed the IMSF of all of the models for the intersection between the 0.020 mag contour level of the reddening dispersion surface [Fig. (3a)] and the exponent  $\alpha$  used in

the models ( $-2.5, -2.0, -1.5, -1.0$ ). In addition, we computed the IMSF of all models outside that contour having a color-excess dispersion within 0.003 mag of 0.020 mag. We also computed some other IMSFs that do not have the abovementioned characteristics in order to check their appearance. Figures 5(a)–5(c) show some of the more typical IMSFs found. Figure 5(d) shows the IMSF of a model with acceptable behavior at small separations but larger than the required reddening dispersion. Figure 5(e) shows the IMSF most similar to the one obtained for NGC 2516. The analysis of the computed IMSF shows that, while their general be-

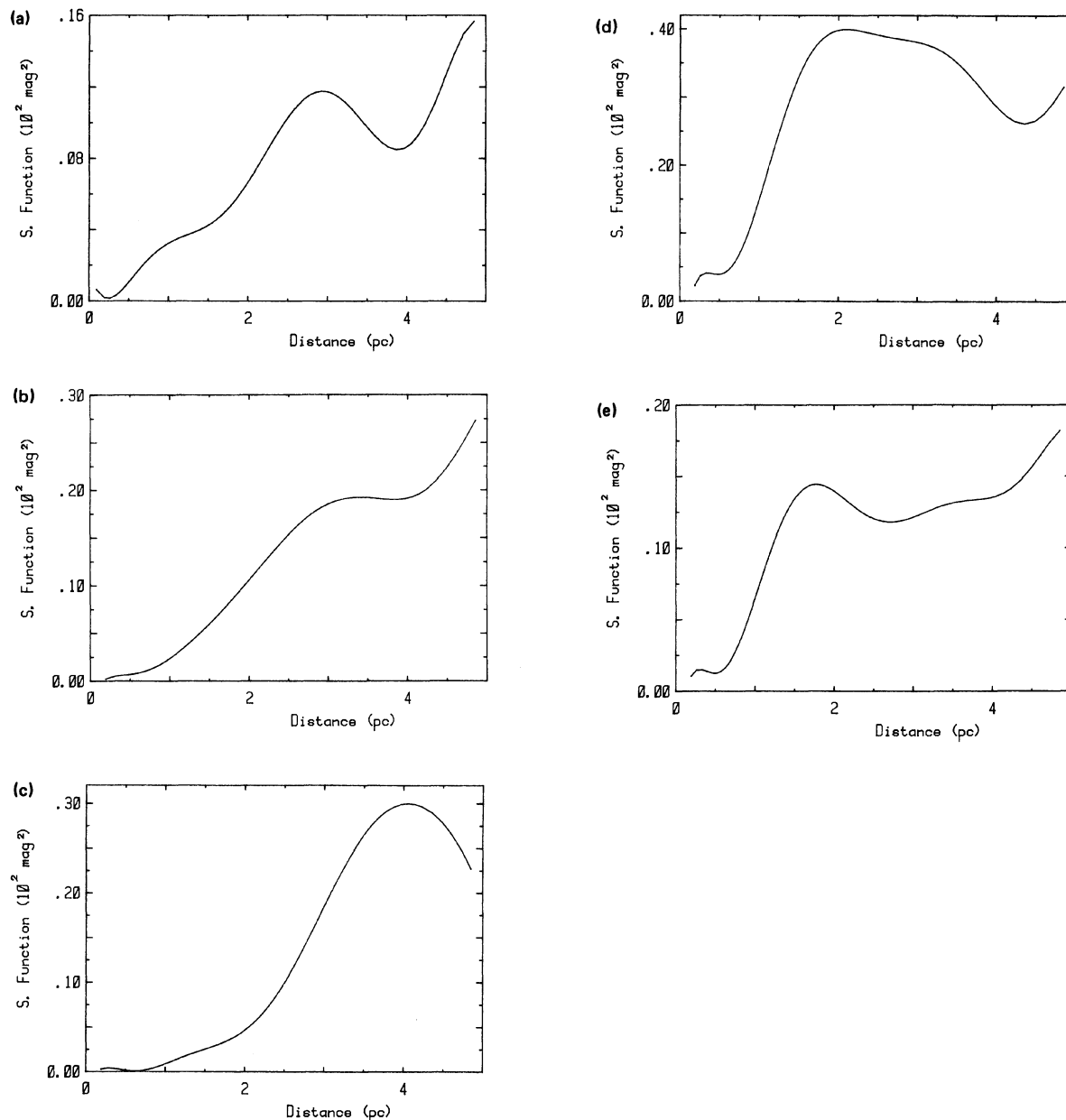


FIG. 5. (a) IMSF for a 12 cloud model with parameters  $\alpha = -1.5, \beta = -1.34$ . The units are the same as in Fig. 1. The reddening dispersion of the model is 0.016 mag. (b) Same as (a) for a seven cloud model with parameters  $\alpha = -2.0, \beta = -2.2$ . The reddening dispersion is 0.21 mag. (c) Same as (a) for a nine cloud model with parameters  $\alpha = -2.5, \beta = -2.5$ . The reddening dispersion is 0.019 mag. (d) The IMSF for a 23 cloud model with parameters  $\alpha = -2.0, \beta = -1.0$ . The reddening dispersion is 0.034. (e) The IMSF for a 14 cloud model with parameters  $\alpha = -2.5, \beta = -3.0$ . The reddening dispersion is 0.021 (see the text).

havior is not strongly affected by the changes in  $\alpha$  and  $\beta$ , the gradient in the neighborhood of 1 pc depends upon the average size of the clouds in the model.

### c) The Dust Distribution

Knowledge of the position and physical characteristics of each cloud makes it possible to construct a halftone image (shaded contour plot) of the dust-distribution model. Figures 6(a-e) [Plates 53-57] show the features of the models whose IMSF are presented.

## V. DISCUSSION

The results obtained do not fully match the IMSF of NGC 2516. The question is why. Before trying to answer it, one detail must be taken into account. It concerns the fixed parameters introduced in Sec. III to set the limits for the acceptable cloud region. One might think that a change in these parameters could change the results in a favorable way. Changes in the fixed parameters would affect the model modifying the features of the acceptable cloud region. In other words, the distribution of cloud masses, central densities, and typical radii would be affected. However, the behavior of the IMSF with changes in  $\alpha$  and  $\beta$  (that also change the distributions) shows that these fixed parameters are not closely related to the features of the IMSF.

In Sec. II, we pointed out two relevant features of the observed IMSF of NGC 2516. Some of our models approximately match the second of these features, the gradient in the neighborhood of 1 pc. In general, these successful models belong to the region of the  $\alpha, \beta$  plane that has mean typical radius less than 5 pc and a mean number of clouds per model greater than 10 (approximate values required to match the observed reddening dispersion of NGC 2516). Consequently, they produce a color-excess dispersion larger than that observed. Hence, we must try to join two features that the models show separately; a large number of small clouds and a moderate color-excess dispersion.

The model presented in Fig. 5(e) can serve to improve our insight in this matter. This model has more clouds than is usual for the  $\alpha$  and  $\beta$  parameters used, but the resulting color-excess dispersion is less than the average for the same number of clouds. However, in looking at Fig. 6(e) we see that the distribution of clouds for this model is very particular. Most of the small clouds occur in a group. This could be a solution to the disagreement mentioned above; small clouds forming groups of clouds. The effect of the clumping of clouds will be the homogenization of photometric properties of the sky at intermediate and large separations. Effectively, the photometric properties of a cluster of clouds at

distances on the order of the cluster size will be similar to the effect of a cloud of the same size. However, the existence of structure in such a large cloud will give the necessary differences in reddening at small distances. Consequently, the slope of the IMSF near 1 pc would be appropriate, and the dispersion in color excess would be less than that resulting for nongrouped clouds.

Regarding the first feature noted in Sec. II, our models do not provide an adequate fit. None of the models shows an oscillating behavior in the IMSF. In Paper I it is shown that the oscillating behavior is related to preferential distances between the dust concentrations. The impossibility, numerically tested, of building such an IMSF with a uniform distribution of clouds strengthens that conclusion. Hence, the solution to this disagreement must be some kind of cloud distribution that favors the appropriate separations. In addition, this kind of solution will also contribute to lowering the resulting color-excess dispersion.

## VI. CONCLUSION

(a) The slope of the observed IMSF of NGC 2516 in the neighborhood of 1 pc can be statistically matched by clouds having typical average sizes of about 3 pc. However, the computed models that have this characteristic provide a color-excess dispersion larger than required. A solution to this disagreement could be the clumping of individual clouds into a complex of clouds.

(b) The oscillating behavior of the observed IMSF of NGC 2516 cannot be matched by our models. A solution to this behavior seems to be some kind of periodicity in the positions of the complexes.

Conclusions (a) and (b) converge to the following general conclusion. Disregarding the fact that the region of the sky under study is rather small, the concentrations of gas and dust do not appear to be stochastically located.

The numerical test of our propositions, together with similar studies of other sky regions, seem to be worthwhile possibilities for further investigation.

It is a pleasure to acknowledge Mr. R. Leonardi and C. C. G. Ginestet for their assistance at the computer. It is also a pleasure to acknowledge Mr. G. E. Sierra for assistance in the photographic laboratory. Various grants from the Comisión de Investigaciones Científicas de la Provincia de Buenos Aires, the Consejo Nacional de Investigaciones Científicas y Técnicas, and the Secretaría de Estado de Ciencia y Tecnología that allowed the purchase of the HP 1000/F computer are gratefully acknowledged.

## REFERENCES

- Bhatt, H. C., Rowse, D. P., and Williams, I. P. (1984). *Mon. Not. R. Astron. Soc.* **209**, 69.
- Chandrasekhar, S., and Münch, G. (1952). *Astrophys. J.* **115**, 103.
- Clocchiatti, A., and Marraco, H. G. (1986). *Rev. Mex. Astron. Astrofis.* **12**, 264.
- Cox, A. N. (1955). *Astrophys. J.* **121**, 628.
- Dachs, J. (1970). *Astron. Astrophys.* **5**, 312.
- Eggen, O. J. (1972). *Astrophys. J.* **173**, 63.
- Evans, D. S., Menzies, A., Stoy, R. H., and Wayman, P. A. (1961). *R. Obs. Bull.* No. 48.
- Feinstein, A., Marraco, H. G., and Mirabel, I. (1973a). *Astron. Astrophys. Suppl.* **9**, 233.
- Feinstein, A., Marraco, H. G., and Muzzio, J. C. (1973b). *Astron. Astrophys. Suppl.* **12**, 331.
- Feinstein, A., and Marraco, H. G. (1971). *Bol. Asoc. Arg. Astron.* **16**, 16.
- Knude, J. (1981). *Astron. Astrophys.* **98**, 74.

- Krzemiński, W., and Serkowski, K. (1967). *Astrophys. J.* **147**, 988.  
Lucke, P. B. (1978). *Astron. Astrophys.* **64**, 367.  
Marraco, H. G. (1975). Unpublished thesis, Facultad de Ciencias Astronómicas y Geofísicas, Universidad Nacional de La Plata.  
Mathis, J. S., and Wallenhorst, S. G. (1981). *Astrophys. J.* **244**, 483.  
McCutcheon, W. H. (1982). *Astrophys. J.* **256**, 139.  
Münch, G. (1952). *Astrophys. J.* **116**, 575.  
Reddish, V. C. (1971). *Nature* **232**, 40.  
Reddish, V. C., and Sloan, C. (1971). *The Observatory* **91**, No. 981, 70.  
Scheffler, H. (1967). *Z. Astrophys.* **65**, 60.  
Serkowski, K. (1958). *Acta Astron.* **8**, 135.  
Serkowski, K. (1968). *Astrophys. J.* **154**, 115.

(a)



FIG. 6. (a) A shaded contour plot of color excess distribution of the model whose IMSF is presented in Fig. 5(a). The region of the sky represented is  $10 \text{ pc} \times 10 \text{ pc}$  on NGC 2516. The contour interval in color excess is approximately 0.014 mag. The darkest regions correspond to a color excess of about 0.20 mag. The clearest ones correspond to a color excess of about 0.06 mag. The centers of seven of the 12 clouds of the model fall within the frame.

A. Clocchiatti and H. Marraco (see page 1136)

(b)

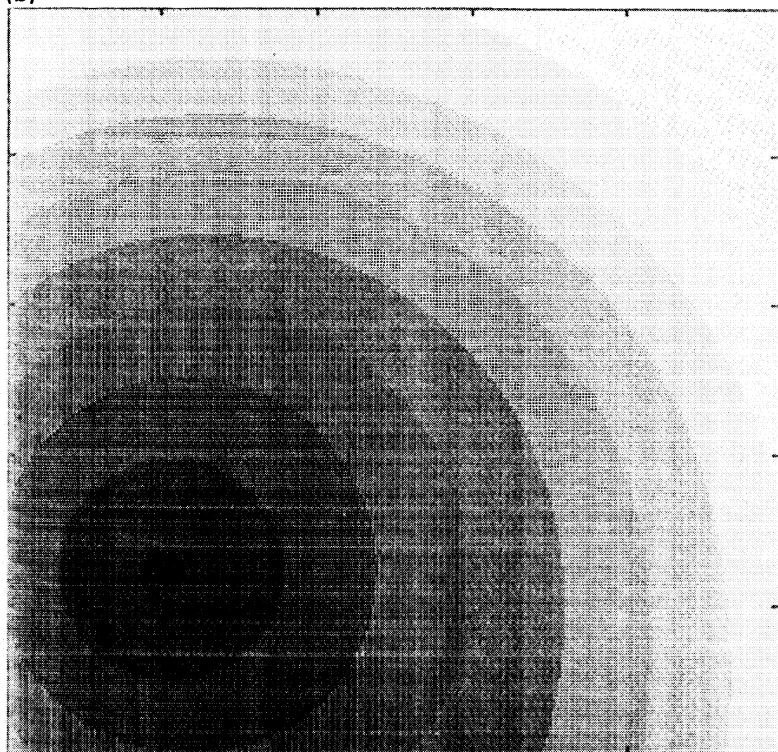


FIG. 6. (b) Same as (a) for the model whose IMSF is presented in Fig. 5(b). The contour interval in color excess is approximately 0.016 mag. The darkest regions correspond to a color excess of about 0.19 mag. The clearest ones correspond to a color excess of about 0.02 mag. The centers of five of the seven clouds of this model fall within the frame.

A. Clocchiatti and H. Marraco (see page 1136)

(c)

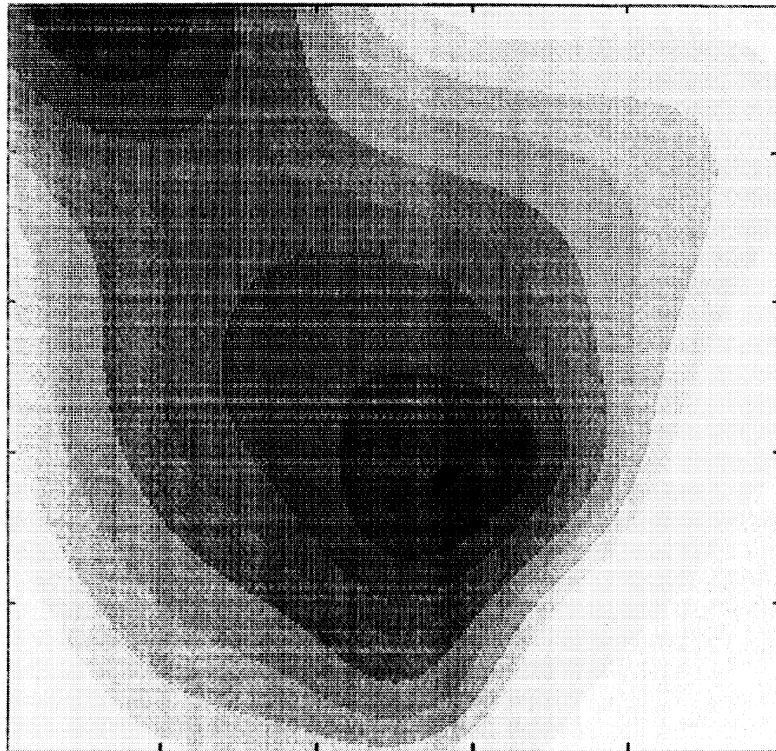


FIG. 6. (c) Same as Fig. 6(a) for the model whose IMSF is presented in Fig. 5(c). The contour interval in color excess is approximately 0.015 mag. The darkest regions correspond to a color excess of about 0.015 mag. The clearest ones correspond to a color excess of about 0.01 mag. The centers of seven of the nine clouds of the model fall within the frame.

A. Clocchiatti and H. Marraco (see page 1136)

(d)



FIG. 6. (d) Same as Fig. 6(a) for the model whose IMSF is presented in Fig. 5(d). The contour interval in color excess is approximately 0.017 mag. The darkest regions correspond to a color excess of about 0.20 mag. The clearest ones correspond to a color excess of about 0.04 mag. The centers of 17 of the 23 clouds of the model fall within the frame.

A. Clocchiatti and H. Marraco (see page 1136)

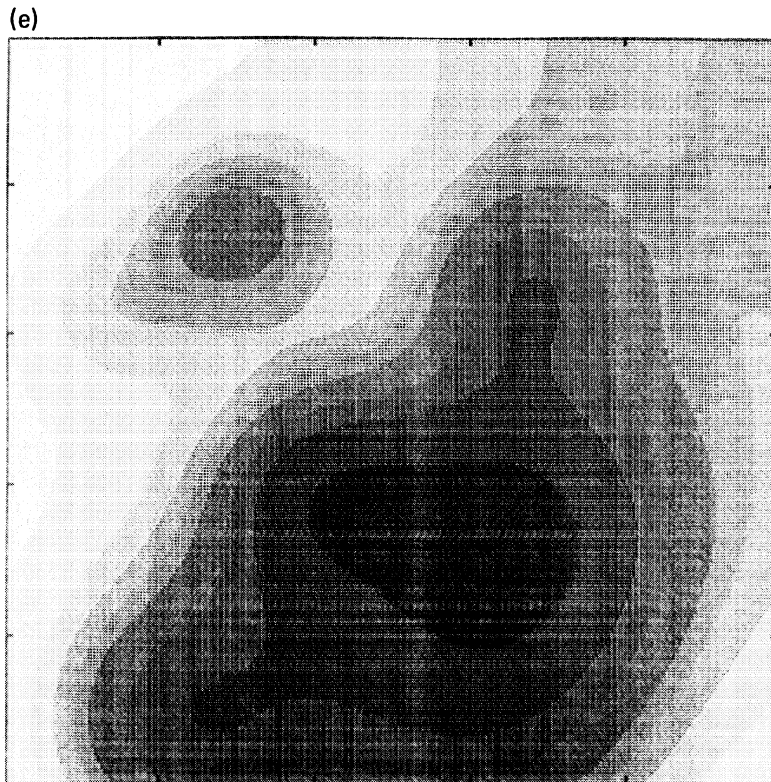


FIG. 6. (e) Same as Fig. 6(a) for the model whose IMSF is presented in Fig. 5(e). The contour interval in color excess is approximately 0.014 mag. The darkest regions correspond to a color excess of about 0.18 mag. The clearest ones correspond to a color excess of about 0.04 mag. The centers of ten of the 14 clouds of the model fall within the frame.

A. Clocchiatti and H. Marraco (see page 1136)